# Activity Coefficients of an Electrolyte in a Mixture with a High Density Neutral Component†

**C. W. Outhwaite**

Department of Applied Mathematics, University of Sheffield, Sheffield S3 7RH, U.K.

**L. B. Bhuiyan**

Laboratory of Theoretical Physics, Department of Physics, University of Puerto Rico, San Juan, Puerto Rico 00931-3343

**V. Vlachy and B. Hribar-Lee**

Faculty of Chemistry and Chemical Technology, University of Ljubljana, Aškerčeva 5, 1000 Ljubljana, Slovenia

Activity coefficients for the primitive model electrolyte, containing a high concentration of neutral hard spheres, are calculated for the modified Poisson−Boltzmann (MPB), hypernetted chain (HNC), and mean spherical approximation (MSA) theories. Comparisons are made with Monte Carlo (MC) simulation results for a 1:1 electrolyte having a common ion diameter with the neutral molecule diameter equal or different to that of the ions. Various electrolyte concentrations are treated with the overall packing fraction held fixed at 0.3. A very good agreement with simulation for the MPB theory is found for the charging parameter approach, that via the virial route being less accurate. The MSA activity coefficients via the energy route also give a good representation of the simulation values, while the HNC theory is adequate only for low volume fractions of added neutral particles.

## Introduction

Debye and Hückel (DH)[1] initiated the first fundamental approach to determine the thermodynamic properties of strong electrolytes. Subsequently, their approach has become the basis of numerous theoretical and practical applications.[2–10] Because of the inherent approximations in their theory and electrolyte model, the classical DH approach is restricted mainly to uni-univalent salts at low concentrations. The basic model developed from their approach, which has been the subject of numerous investigations, is the restricted primitive model (RPM). This model is a system of charged hard spheres of equal diameter moving in a dielectric medium of constant permittivity. Allowing the cations and anions to have unequal sizes gives the primitive model (PM). An extensive investigation of the applicability of the PM to analyze the thermodynamic properties of various salts has recently been carried out using Monte Carlo (MC) simulations.[11]

A principal objection to the use of the PM is the neglect of the molecular nature of the solvent. A first step to mimic the solvent molecular structure is the solvent primitive model (SPM), where the solvent molecules are treated as uncharged hard spheres moving in a dielectric medium.[12] The solvent hard spheres, because of their large concentrations, tend to drive the structural properties of the solution leading to damped oscillatory ion and solvent radial distribution functions. The influence of the hard sphere solvent on structural properties in the SPM is also observed in inhomogeneous situations such as the planar electric double layer.[13–15]

An alternate interpretation of the uncharged hard spheres is that of a neutral cosolute. This has enormous relevance for many industrial chemical processes and biological sciences. Many biologically significant ion−ion or ion−protein reactions take place in solutions with a *crowded* environment of inert macromolecules. Terms such as *macromolecular crowding* are used to describe the effects of the addition of neutral cosolutes on the equilibrium and nonequilibrium behavior of the solution.[16–19] Lack of available space for reacting ions in the solution can lead to important consequences such as protein precipitation, protein folding, and oligomerization.[17] Mixtures of electrolytes and neutral cosolutes at low to moderate concentrations of the components have been recently studied[20–25] using MC simulations and other analytical approaches such as the symmetric Poisson−Boltzmann (SPB) theory,[26] the modified Poisson−Boltzmann (MPB) theory,[27,28] and the hypernetted chain (HNC) integral equation.[4,29] One interesting finding in these studies is the phenomenon of like-charge attraction that is manifest at sufficiently high concentrations of the neutral species. Further improvements in the charged fluid models, by the incorporation of dipoles and higher-order multipoles, are required to treat polarization effects. Such models provide a theoretical and simulation challenge.

Recently Lamperski and Płuciennik[30] have calculated, using MC simulations, the activity coefficients for a 1:1 SPM electrolyte at various electrolyte concentrations. They considered a high concentration of neutral particles, which mimics a crowded environment, at a constant value of the total packing fraction equal to 0.3. Comparisons were also made with the mean spherical approximation (MSA)[31] and the SPB theory. We compare here the results of the MPB theory and the HNC and MSA integral equations with these MC results. The MPB

† Part of the "Sir John S. Rowlinson Festschrift".

* Corresponding author. E-mail: c.w.outhwaite@sheffield.ac.uk.

10.1021/je100394d 
Published on Web 06/29/2010

improves upon the SPB theory and is found to be in very good agreement with the simulation results. The HNC is seen to be somewhat poor relative to the simulations and other theories at the high packing fraction.

## Model and Theory

The electrolyte model treated in this work is a three-component system of charged hard spheres (cations and anions) of diameter $d$ and uncharged hard spheres of diameter $d_s$, moving in a dielectric continuum of constant permittivity $\varepsilon_r$. For reference we will denote this model by SPM. To compute the activity coefficients of the SPM, we use the MPB, HNC, and MSA approaches. The MPB theory is based on correcting the two approximations inherent in the classical PB theory, namely, the fluctuation and the exclusion volume terms.[28] The basic equation in the MPB approach is Poisson's equation satisfied by the mean electrostatic potential $\Psi_\alpha(r)$ a distance $r$ from the center of a molecule of species $\alpha$, namely

$$\nabla^2\psi_\alpha(r) = -\frac{1}{\varepsilon_0\varepsilon_r}\sum_t e_t\rho_t g_{\alpha t}(r) \tag{1}$$

where $t$ is the sum over the ion species, $\varepsilon_0$ the vacuum permittivity, $\rho_t$ the mean number density of species $t$, and $g_{\alpha t}(r)$ the radial distribution function for two molecules of species $\alpha$ and $t$ a distance $r$ apart. We consider the special case of a 1:1 electrolyte with a common ion diameter $d$ so that $\psi_\alpha(r) = 0$ for the neutral molecules and $\psi_\alpha(r{:}e_\alpha = 0) = 0$ for the ions. Within the MPB theory an approximate radial distribution function between two ions $i$ and $j$ is[28]

$$g_{ij}(r) = g_{ij}^0(r)\exp\left\{-\left(\frac{1}{2k_BT}\right)[e_jL(u_i) + e_iL(u_j)]\right\} \tag{2}$$

with

$$L(u) = \frac{1}{2(1+y)r}[u(r+d) + u(r-d) + \kappa\int_{r-d}^{r+d} u(R)\,\mathrm{d}R] \tag{3a}$$

$$g_{ij}^0(r) = g_{ij}(r{:}e_i = e_j = 0) \tag{3b}$$

$$u_\alpha(r) = r\psi_\alpha(r) \tag{3c}$$

where $y = \kappa d$, $\kappa = [(1/k_BT\varepsilon_0\varepsilon_r)\sum_t e_t^2\rho_t]^{1/2}$ is the DH parameter, $k_B$ is the Boltzmann constant, $T$ the absolute temperature, and $g_{ij}^0(r)$ is the exclusion volume term. The PB equation is obtained by putting $d = 0$ in $L(u)$ and replacing $g_{ij}^0(r)$ by the unit step function.

Combining the result for $g_{ij}(r)$ with Poisson's equation gives, for an ion $\alpha$,

$$\frac{1}{r}\frac{d^2u_\alpha}{dr^2} = -\frac{1}{\varepsilon_0\varepsilon_r}\sum_t e_t\rho_t g_{\alpha t}^0(r)\exp\left\{-\left(\frac{1}{2k_BT}\right)[e_\alpha L(u_t) + e_tL(u_\alpha)]\right\} \qquad r > d \tag{4}$$

$$u_\alpha = \left(\frac{r}{d}\right)u_\alpha(d) - \frac{e_\alpha}{4\pi\varepsilon_0\varepsilon_r}(r-d) \qquad 0 < r < d \tag{5}$$

To obtain a closed system of equations for $u_\alpha$ we approximate $g_{ij}^0(r)$ by the Percus−Yevick (PY) uncharged hard sphere value for mixtures,[32] together with the generalization to mixtures[33] of the Verlet and Weis[34] (VW) correction for a single component system. Note that $g_{ij}^0(r)$ is not the pure uncharged hard sphere radial distribution function but the radial distribution function of two uncharged ions moving in a sea of fully charged ions and neutral molecules. Similarly, the radial distribution function of the neutral molecules is approximated by the PY + VW value for mixtures. The mean electrostatic potential and its first derivative are continuous for $r > 0$ with $u_\alpha \to 0$ as $r \to \infty$.

The HNC theory is based on the Ornstein−Zernike equation

$$g_{\alpha\beta} - 1 = c_{\alpha\beta} + \sum_t \rho_t\int c_{\alpha t}(g_{t\beta} - 1)\,\mathrm{d}V_t \tag{6}$$

with the closure

$$\ln g_{\alpha\beta} = -u_{\alpha\beta}/k_BT + g_{\alpha\beta} - 1 - c_{\alpha\beta} \tag{7}$$

where the sum in $t$ is over all species, $c_{\alpha\beta}$ is the direct correlation function, and $u_{\alpha\beta}$ is the spherically symmetric pair potential for species $\alpha$ and $\beta$. Combining the closure $c_{\alpha\beta} = -u_{\alpha\beta}/k_BT$ with the Ornstein−Zernike equation leads to the MSA integral equation. The MSA equation has proved to be very useful as it has an analytical solution and provides closed form thermodynamic properties.

## Results and Discussion

The MPB equation for the mean electrostatic potential was solved numerically using the previously developed quasi-linearization iteration technique,[35] while the PY uncharged hard sphere radial distribution function was determined by Perram's[36] technique which is based on the work of Baxter.[37] Solving for the mean electrostatic potential means that the iteration technique is robust and requires few iterations for convergence. The virial and the charging (or coupling) parameter routes were considered for calculating the MPB activity coefficient. In the charging route the individual activity coefficient $\gamma_\alpha$ for an ion $\alpha$ is derived from[26]

$$\ln\gamma_\alpha = \ln\gamma_\alpha^{HS} + \ln\gamma_\alpha^{el} \tag{8}$$

where $\ln\gamma_\alpha^{HS}$ is the hard sphere contribution, and the electrical contribution is given by

$$\ln\gamma_\alpha^{el} = \frac{e_\alpha}{k_BT}\int_0^1\left[\psi_\alpha(d,\lambda) - \frac{4\pi\lambda e_\alpha}{\varepsilon_0\varepsilon_r d}\right]\mathrm{d}\lambda \tag{9}$$

The expression for the electrical activity corresponds to that derived by the Güntelberg charging process. To calculate $\ln\gamma_\alpha^{HS}$ we use the uncharged hard sphere individual activity coefficient derived by Ebeling and Scherwinski[38](ES). Lamperski and Płuciennik have demonstrated the accuracy of the ES formula for the present SPM parameters. In the virial route a version of the Gibbs−Duhem equation for three species[39] provides a

**Table 1. Natural Logarithm ln $\gamma_\pm$ of the Mean Activity Coefficient of the Electrolyte and of the Neutral Species ln $\gamma_s$ for Equal Ion and Neutral Diameters of (0.3, 0.4, and 0.5) nm at Varying Electrolyte Concentrations $c_{elec}$ with $\eta = 0.3$[a]**

| | $d = d_s = 0.3$ nm | | | | | $d = d_s = 0.4$ nm | | | | | $d = d_s = 0.5$ nm | | | | |
|---|---|---|---|---|---|---|---|---|---|---|---|---|---|---|---|
| $c_{elec}$ | ln $\gamma_\pm$ | | | | ln $\gamma_s$ | ln $\gamma_\pm$ | | | | ln $\gamma_s$ | ln $\gamma_\pm$ | | | | ln $\gamma_s$ |
| mol·dm$^{-3}$ | $MSA_e$ | $MPB_{ch}$ | HNC | MC | ES | $MSA_e$ | $MPB_{ch}$ | HNC | MC | ES | $MSA_e$ | $MPB_{ch}$ | HNC | MC | ES |
| 0.05 | 4.65 | 4.64 | 4.91 | 4.6507 | 4.87 | 4.67 | 4.65 | 5.00 | 4.6645 | 4.87 | 4.68 | 4.66 | 5.06 | 4.6868 | 4.87 |
| 0.1 | 4.58 | 4.56 | 4.84 | 4.5681 | 4.87 | 4.60 | 4.58 | 4.93 | 4.6010 | 4.87 | 4.62 | 4.60 | 4.99 | 4.6214 | 4.87 |
| 0.25 | 4.47 | 4.43 | 4.71 | 4.4323 | 4.87 | 4.50 | 4.47 | 4.82 | 4.4935 | 4.87 | 4.53 | 4.50 | 4.90 | 4.5135 | 4.87 |
| 0.50 | 4.36 | 4.31 | 4.59 | 4.3288 | 4.87 | 4.41 | 4.37 | 4.72 | 4.3875 | 4.87 | 4.46 | 4.41 | 4.81 | 4.4354 | 4.87 |
| 1 | 4.24 | 4.17 | 4.46 | 4.1982 | 4.87 | 4.32 | 4.26 | 4.61 | 4.2861 | 4.87 | 4.37 | 4.32 | 4.72 | 4.3353 | 4.87 |
| 1.5 | 4.16 | 4.08 | 4.37 | 4.1147 | 4.87 | 4.26 | 4.19 | 4.54 | 4.2123 | 4.87 | 4.32 | 4.26 | 4.66 | 4.2765 | 4.87 |
| 2 | 4.11 | 4.02 | 4.31 | 4.0466 | 4.87 | 4.21 | 4.14 | 4.49 | 4.1634 | 4.87 | 4.29 | 4.22 | 4.61 | 4.2269 | 4.87 |
| 2.5 | 4.06 | 3.97 | 4.26 | 3.9965 | 4.87 | 4.18 | 4.10 | 4.45 | 4.1179 | 4.87 | 4.26 | 4.19 | 4.58 | 4.1934 | 4.87 |
| 3 | 4.03 | 3.93 | 4.22 | 3.9637 | 4.87 | 4.15 | 4.06 | 4.42 | 4.0912 | 4.87 | 4.24 | 4.16 | 4.55 | 4.1437 | 4.87 |

[a] Under the ln $\gamma_\pm$ column, $MSA_e$ denotes the energy route, $MPB_{ch}$ the charging parameter route, and HNC via eq 10 and MC the simulation results of ref 30, strictly only accurate to three significant figures. The ES results for ln $\gamma_s$ are calculated from the formula of ref 38.

procedure for calculating the mean activity coefficient $\gamma_\pm$ of the electrolyte.

The numerical solution of the HNC equation was also determined using a previously developed technique.[40] Because of the long-range nature of the Coulomb interactions, the integral equations have first to be renormalized before being solved using a fast Fourier transform technique. The activity coefficient in the HNC approach is calculated via[41]

$$\ln \gamma_\alpha = -\sum_t \rho_t c^0_{\alpha t}(0) + 0.5 \sum_t \rho_t \int [(g_{\alpha t} - 1)(g_{\alpha t} - 1 - c_{\alpha t})]\, dV_t \quad (10)$$

where $c^0_{\alpha t}(0)$ is the Fourier transform of the short-range part of the direct correlation function evaluated at $k = 0$. Note that eq 10 is only valid for the HNC equation. The MSA activity coefficients were calculated from the analytical formula derived via the energy route.[38,42,43] This route provides the most accurate MSA thermodynamic properties.

Calculations were carried out for the SPM parameters corresponding to the simulation results of Lamperski and Płuciennik with $T = 298.15$ K and $\varepsilon_r = 78.5$. These simulations were done using a modification of the grand canonical Monte Carlo (GCMC) techniques called the inverse GCMC method,[44] where unlike in the GCMC, the activity coefficient can be evaluated for a given solution concentration. This allows a straightforward calculation of the individual activity coefficients of the constituent species in a mixture. Simulations were performed at the constant packing fraction $\eta = 0.3$ where

$$\eta = (\pi/6) \sum_t \rho_t d_t^3 \quad (11)$$

Keeping $\eta$ constant means that, as the electrolyte concentration $c_{elec}$ is changed, the neutral species concentration also changes.

We first consider the situation when all of the diameters are equal with $d = d_s = (0.3, 0.4, \text{or } 0.5)$ nm. Table 1 gives the activity results for the electrolyte and neutral species at various electrolyte concentrations, with the corresponding electrolyte plots shown in Figure 1. For these parameters the neutral species ln $\gamma_s$ are essentially independent of the electrolyte concentration and diameter $d$. In the limit of zero electrolyte concentration the electrolyte ln $\gamma_\pm$ tends to that of the neutral species as the solution then becomes a one-component hard sphere system. At all three diameter values the MPB activity coefficient derived from the charging route agrees with those of the MC. The MSA

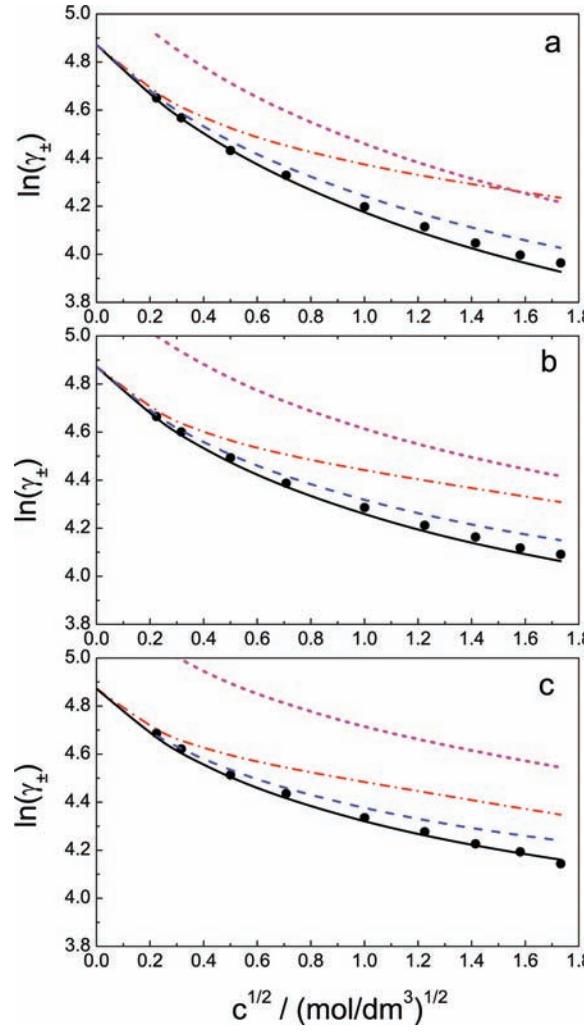


**Figure 1.** Natural logarithm ln $\gamma_\pm$ of the mean activity coefficient of the electrolyte for $d = d_s$. Graphs a, b, and c are for diameters of (0.3, 0.4, and 0.5) nm, respectively. Solid line, MPB charging; dashed line, MSA energy; dashed−dotted line, MPB virial; dotted line, HNC eq 10; symbols, MC.[30]

is in good agreement with the MC values, only beginning to deviate from them at the higher electrolyte concentrations. The MPB virial activity coefficient is less accurate than that of the MSA, while the HNC activity coefficient is comparatively poorer even at low $c_{elec}$. The deviation of the HNC results from simulation is not entirely unexpected as the overestimation of the HNC osmotic coefficient in the presence of a neutral component has been seen earlier.[22,25] The HNC closure is a

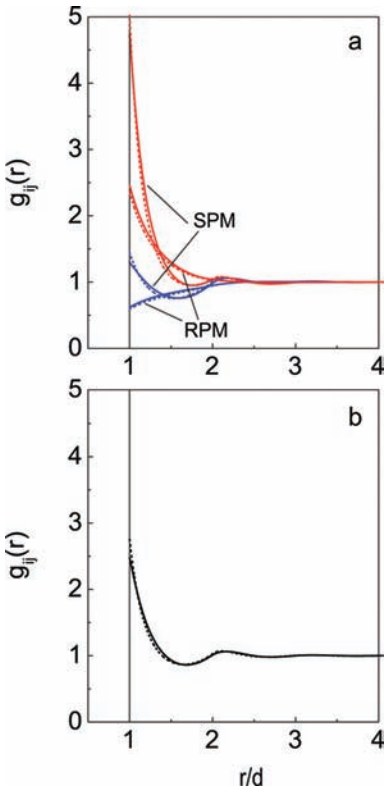


**Figure 2.** RPM and SPM radial distribution functions $g_{ij}(r)$ with $d = d_s = 0.4$ nm and $c_{elec} = 2$ mol·dm$^{-3}$ and for SPM, neutral species concentration = 10.866 mol·dm$^{-3}$. Solid line, MPB; dotted line, HNC. Panel a, ion−ion distribution; Panel b, ion−neutral species distribution.

very good approximation for Coulomb interactions, but it underperforms for harsh, short-range, forces. Note that the concentrations of the components used here are much bigger than those in the earlier works,[22–24] and hence it is not surprising to see the deviations displayed by the HNC theory.

Figure 2a illustrates, for $d = 0.4$ nm and $c_{elec} = 2$ mol·dm$^{-3}$, the influence the uncharged hard spheres have on the MPB and HNC ion radial distribution functions relative to those of the RPM. At this value of $c_{elec}$ the value of $y$ is equal to 1.8595 so that in the RPM small damped charge oscillations occur in $g_{ij}(r)$[28] which are too small to be seen in the figure. Also for small ion separation $g_{ij}(r)$ predicts the expected like ion repulsion or unlike ion attraction. When the neutral species is present having a concentration of 10.866 mol·dm$^{-3}$, corresponding to $\eta = 0.3$, a pronounced structure occurs in $g_{ij}(r)$. The high density of the neutral species drives the ion structure and leads to the interesting phenomenon of like ion attraction arising from depletion effects,[45] with $g_{ii}(d) > 1$ and a small maximum in $g_{ij}(r)$ at approximately two molecular diameters. Panel b of Figure 2 shows the ion−neutral species distribution corresponding to the SPM parameters of panel a. The neutral−neutral species distribution is not shown as the HNC distribution is very close to the ion−neutral species distribution,[22] while the MPB theory does not differentiate between the two distributions. The structural similarities between the ion and the neutral species distributions can be clearly seen. The HNC and MPB radial distributions for both the RPM and the SPM are quite close overall. However, a closer inspection reveals the HNC contact values of the various distributions to be somewhat bigger than those of the corresponding MPB theory. This seems to be one of contributing factors to the higher HNC osmotic coefficients and hence the higher activity coefficients noted above.

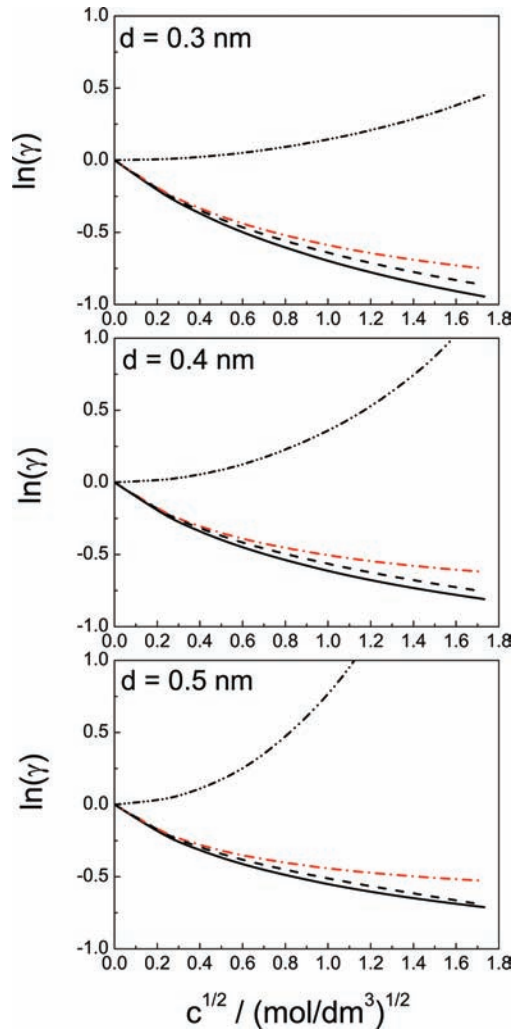


**Figure 3.** MPB ln $\gamma_{\pm}^{el}$ from the charging route for the SPM and RPM electrolytes, the DH ln $\gamma_{\pm}^{el}$ and corresponding ln $\gamma^{HS}$ for the RPM, with $d = d_s = (0.3, 0.4, \text{and } 0.5)$ nm. Solid line, SPM MPB; dashed line, RPM MPB; dashed−dotted line, DH; dashed−two dots line, RPM uncharged hard sphere.

The equal size situation, $d_s = d$, provides a contact with the RPM electrolyte mean activity coefficients at the same electrolyte concentrations as the SPM. Figure 3 compares the SPM ln $\gamma_{\pm}^{el}$ for the MPB theory and the corresponding RPM ln $\gamma_{\pm}^{el}$ for the MPB theory and DH theory with size. The graphs illustrate the fairly small influence the SPM high packing fraction of the neutral species has on the value of the RPM

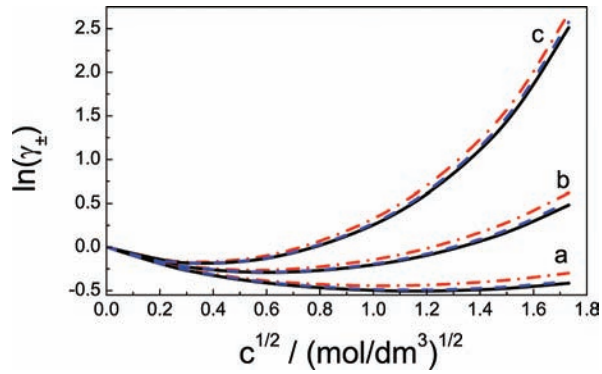


**Figure 4.** RPM ln $\gamma_{\pm}$ for the MPB, MSA, and DH theories at $d = (0.3, 0.4, \text{and } 0.5)$ nm. Solid line, MPB charging; dashed−dotted line, MSA energy; dashed line, DH.

**Table 2. Natural Logarithm ln $\gamma_\pm$ of the Mean Activity Coefficient of the Electrolyte and of the Neutral Species ln $\gamma_s$ for the Ion Diameter $d$ = 0.4 nm and the Neutral Diameter $d_s$ Taking the Values (0.3 and 0.5) nm at Varying Electrolyte Concentrations $c_{elec}$ with $\eta$ = 0.3[a]**

| | $d$ = 0.4 nm, $d_s$ = 0.3 nm | | | | | $d$ = 0.4 nm, $d_s$ = 0.5 nm | | | | |
|---|---|---|---|---|---|---|---|---|---|---|
| $c_{elec}$ | ln $\gamma_\pm$ | | | | ln $\gamma_s$ | ln $\gamma_\pm$ | | | | ln $\gamma_s$ |
| mol·dm$^{-3}$ | $MSA_e$ | $MPB_{ch}$ | HNC | MC | ES | $MSA_e$ | $MPB_{ch}$ | HNC | MC | ES |
| 0.05 | 8.28 | 8.27 | 8.90 | 8.3259 | 4.86 | 3.11 | 3.09 | 3.31 | 3.1037 | 4.89 |
| 0.1 | 8.19 | 8.17 | 8.80 | 8.1979 | 4.84 | 3.05 | 3.03 | 3.25 | 3.0417 | 4.90 |
| 0.25 | 8.01 | 7.98 | 8.61 | 7.9975 | 4.80 | 2.98 | 2.95 | 3.18 | 2.9671 | 4.95 |
| 0.50 | 7.79 | 7.75 | 8.36 | 7.7784 | 4.74 | 2.94 | 2.90 | 3.13 | 2.9182 | 5.04 |
| 1 | 7.43 | 7.38 | 7.97 | 7.4055 | 4.60 | 2.95 | 2.88 | 3.13 | 2.9021 | 5.20 |
| 1.5 | 7.11 | 7.06 | 7.62 | 7.0683 | 4.47 | 2.99 | 2.92 | 3.17 | 2.9461 | 5.37 |
| 2 | 6.81 | 6.76 | 7.29 | 6.7451 | 4.33 | 3.05 | 2.97 | 3.23 | 2.9932 | 5.54 |
| 2.5 | 6.52 | 6.47 | 6.98 | 6.4551 | 4.20 | 3.12 | 3.03 | 3.30 | 3.0497 | 5.71 |
| 3 | 6.25 | 6.19 | 6.67 | 6.1844 | 4.07 | 3.19 | 3.10 | 3.38 | 3.1116 | 5.88 |

[a] The notation is as in Table 1.

**Table 3. Natural Logarithm ln $\gamma_\pm$ of the Mean Activity Coefficient of the Electrolyte and of the Neutral Species ln $\gamma_s$ for a Neutral Diameter $d_s$ = 0.4 nm and Ion Diameters of (0.3 and 0.5) nm at Varying Electrolyte Concentrations $c_{elec}$ with $\eta$ = 0.3[a]**

| | $d$ = 0.3 nm, $d_s$ = 0.4 nm | | | | | $d$ = 0.5 nm, $d_s$ = 0.4 nm | | | | |
|---|---|---|---|---|---|---|---|---|---|---|
| $c_{elec}$ | ln $\gamma_\pm$ | | | | ln $\gamma_s$ | ln $\gamma_\pm$ | | | | ln $\gamma_s$ |
| mol·dm$^{-3}$ | $MSA_e$ | $MPB_{ch}$ | HNC | MC | ES | $MSA_e$ | $MPB_{ch}$ | HNC | MC | ES |
| 0.05 | 2.76 | 2.74 | 2.90 | 2.7623 | 4.88 | 7.24 | 7.23 | 7.86 | 7.2361 | 4.85 |
| 0.1 | 2.70 | 2.67 | 2.83 | 2.6706 | 4.89 | 7.15 | 7.13 | 7.76 | 7.1516 | 4.83 |
| 0.25 | 2.59 | 2.55 | 2.72 | 2.5770 | 4.92 | 6.95 | 6.92 | 7.54 | 6.9340 | 4.76 |
| 0.50 | 2.51 | 2.46 | 2.62 | 2.4832 | 4.97 | 6.69 | 6.66 | 7.26 | 6.6554 | 4.65 |
| 1 | 2.44 | 2.37 | 2.54 | 2.3993 | 5.06 | 6.26 | 6.21 | 6.77 | 6.2097 | 4.44 |
| 1.5 | 2.41 | 2.33 | 2.51 | 2.3658 | 5.16 | 5.86 | 5.81 | 6.33 | 5.8025 | 4.23 |
| 2 | 2.40 | 2.32 | 2.50 | 2.3478 | 5.25 | 5.48 | 5.43 | 5.91 | 5.4336 | 4.02 |
| 2.5 | 2.42 | 2.32 | 2.51 | 2.3519 | 5.35 | 5.12 | 5.06 | 5.51 | 5.0290 | 3.82 |
| 3 | 2.43 | 2.33 | 2.52 | 2.3614 | 5.45 | 4.76 | 4.71 | 5.11 | 4.6783 | 3.62 |

[a] The notation is as in Table 1.

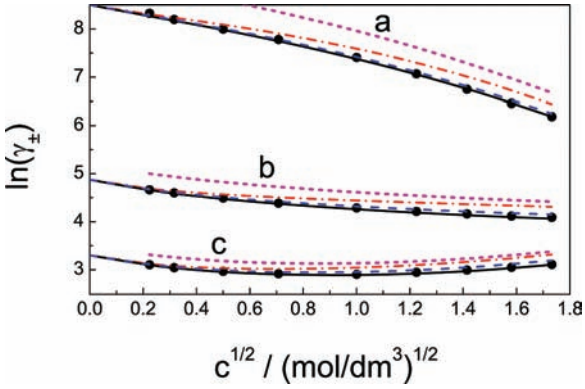


**Figure 5.** SPM ln $\gamma_\pm$ for $d$ = 0.4 nm and $d_s$ = 0.3 nm, curves a; $d_s$ = 0.4 nm, curves b; $d_s$ = 0.5 nm, curves c. Solid line, MPB charging; dashed line, MSA energy; dashed−dotted line, MPB virial; dotted line, HNC eq 10; symbols, MC.[30]

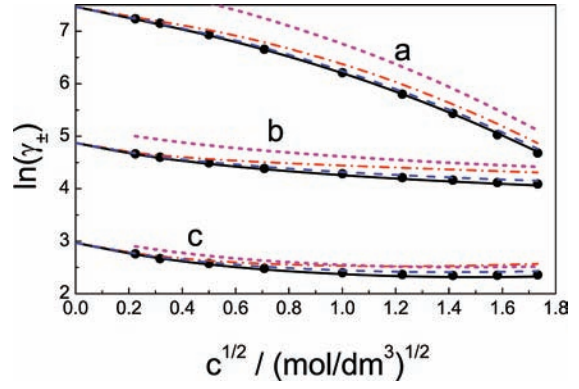


**Figure 6.** SPM ln $\gamma_\pm$ for $d_s$ = 0.4 nm and $d$ = 0.3 nm, curves c; $d$ = 0.4 nm, curves b; $d$ = 0.5 nm, curves a. The remainder of the notation is as in Figure 5.

electrical activity. Also shown is ln $\gamma^{HS}$ corresponding to the RPM electrolyte concentrations. An important feature of the plots is the dominance of the hard sphere contribution to the activity coefficient, which is especially true at higher concentrations. In our calculations we have also found the trend to carry over to the SPM where such dominance of the hard sphere activity is even more substantial. Combining the electrical and hard sphere activity coefficients, see eq 8, gives the overall RPM activity coefficients shown in Figure 4. The MPB activity coefficients for the RPM are known to accurately follow the simulation data.[33] Since the DH and MPB ln $\gamma_\pm^{el}$ in Figure 3 only differ appreciably at the larger $d$ and higher $c_{elec}$, a good estimate of the SPM ln $\gamma_\pm$ can be obtained by adding the SPM ln $\gamma_s$ to the DH electrical value.

Next we compare with the simulation results for the cases where the ion and neutral species differ in size. In Table 2 the activity coefficients are calculated at various electrolyte concentrations for $d$ = 0.4 nm with $d_s$ = 0.3 or 0.5 nm, while Table 3 gives the activity results for $d_s$ = 0.4 nm with $d$ = 0.3 or 0.5 nm. The activity plots corresponding to Tables 2 and 3 are shown in Figures 5 and 6, respectively. Variations in the molecular sizes are seen to have a profound effect on the activity coefficients. Simulation indicates that when $d$ is fixed at 0.4 nm and $d_s$ varies, the ion activity decreases as $d_s$ increases from (0.3 to 0.5) nm. Furthermore, at the smallest value of $d_s$, ln $\gamma_\pm$ decreases monotonically with $c_{elec}$ in contrast to the eventual upturn in ln $\gamma_\pm$ as $c_{elec}$ increases when $d_s$ = 0.5 nm. A somewhat analogous picture holds for $d$ varying with $d_s$ fixed, except that in contrast the ion activity now increases as $d$ increases. The reason for this behavior is that it requires less effort to insert a small sphere into a system of larger spheres than to insert a larger sphere into a system of smaller spheres. Because of the

high density of the uncharged hard spheres relative to the ions, the effect of inserting an ion into the system is dominated by the size of the uncharged molecules. Hence for $d$ fixed and $d_s$ varying, ln $\gamma_\pm$ decreases in the order $d_s < d$, $d_s = d$, and $d_s > d$. Similarly for $d_s$ fixed and $d$ varying, ln $\gamma_\pm$ increases in the order $d < d_s$, $d = d_s$, and $d > d_s$. The activity of the uncharged species for $d \neq d_s$ depends on the electrolyte concentration and is accurately given by the ES formula.

The overall agreement of the theoretical predictions and their comparative behavior parallel closely those of the equal diameter case. As before the MPB activity coefficients calculated via eq 8 are in very good agreement with the corresponding simulation values. The remaining theories tend to overestimate ln $\gamma_\pm$ especially at the higher values of $c_{elec}$, and reduce in accuracy in the order MSA, virial MPB, and HNC, respectively. All of the theories increase in accuracy as the ions reduce in size, plots a → c in the figures, corresponding to the situation when it becomes easier to insert an ion into the solution.

## Conclusion

The MPB activity coefficient derived via eq 8, using the charging process for the electrical contribution and the ES formula for the hard sphere contribution, has been proven to accurately describe the ion activity coefficients at the parameters of the present SPM electrolyte. A good description of the activity coefficients is also given by the MSA analytical results and to a lesser extent at the smaller ion diameters by the HNC theory. Lamperski and Płuciennik had earlier shown that the SPB theory gave an adequate description of ln $\gamma_\pm$. The potential theories thus seem a viable approach to treat more complex electrolytes than the present RPM plus uncharged hard spheres.

Within the potential approaches and the MSA, the calculation of the mean activity coefficient conveniently decouples into a hard sphere part and an electrical part (eq 8). The hard sphere contribution, which tends to dominate, is also well-described by the ES formalism and hence the very good predicted mean activity. In the HNC integral equation approach the closure is applied, on an equal footing, to all of the species. The HNC closure (eq 7) works very well for pure Coulombic systems, but its performance in the presence of a high density neutral species is less successful. Another study is thus required to assess the feasibility of other, for example, mixed (HNC−PY or HNC−MSA), closures for such mixtures. We hope to take up such a project in the near future.

## Literature Cited


(1) Debye, P.; Hückel, E. Zur Theorie der Elektrolyte. 1. Gefrierpunktserniedrigung und vewandte Erscheinungen. *Z. Phys.* **1923**, *24*, 185–206.
(2) Harned, H. S.; Owen, B. B. *The Physical Chemistry of Electrolyte Solutions*, 3rd ed.; Reinhold: New York, 1958.
(3) Friedman, H. L. *Ionic Solution Theory*; Wiley: New York, 1962.
(4) Rasaiah, J. C. *The Liquid State and its Electrical Properties*; Kunhardt, E. E., Christophorou, L. G., Luessen, L. H., Eds.; Plenum Press: New York, 1989; Nato ASI Series Vol. 193, pp 89−142.
(5) Pitzer, K. S. *Activity Coefficients in Electrolyte Solutions*, 2nd ed.; CRC Press: Boca Raton, FL, 1992.
(6) Loehe, J. R.; Donohue, M. D. Recent Advances in Modeling Thermodynamic Properties of Aqueous Strong Electrolyte Systems. *AIChE J.* **1997**, *43*, 180–195.
(7) Bockris, J. O'M.; Reddy, A. K. N. *Modern Electrochemistry*, 2nd ed.; Plenum Press: New York, 1998; Vol. 1, Ionics.
(8) Barthel, J. M. G.; Krienke, H.; Kunz, W. *Physical Chemistry of Electrolyte Solutions*; Baumgärtel, H., Franck, E. U., Grübein, W., Eds.; Springer: New York, 1998.
(9) Robinson, R. A.; Stokes, R. H. *Electrolyte Solutions*, 2nd revised ed.; Dover Publications: Mineola, NY, 2002.
(10) Lamm, G. *The Poisson-Boltzmann Equation, Reviews in Computational Chemistry*; Lipkowitz, K. B., Larter, R., Cundari, T. R., Eds.; Wiley-VCH, John Wiley & Sons, Inc.: New York, 2003; Vol. 19, Chapter 4, pp 147−365.
(11) Abbas, Z.; Ahlberg, E.; Nordholm, S. Monte Carlo Simulations of Salt Solutions: Exploring the Validity of Primitive Models. *J. Phys. Chem. B* **2009**, *123*, 5905–5916.
(12) Grimson, M. J.; Rickayzen, G. Forces between surfaces in electrolyte solutions. *Chem. Phys. Lett.* **1982**, *86*, 71–75.
(13) Zhang, L.; Davis, H. T.; White, H. S. Simulations of Solvent effects on confined electrolytes. *J. Chem. Phys.* **1993**, *98*, 5793–5799.
(14) Patra, C. N.; Ghosh, S. K. Weighted-density-functional theory of electrode-electrolyte interface: beyond the primitive model. *Phys. Rev. E* **1993**, *48*, 1154–1162.
(15) Lamperski, S.; Outhwaite, C. W.; Bhuiyan, L. B. A modified Poisson-Boltzmann analysis of the solvent primitive model electrical double layer. *Mol. Phys.* **1996**, *87*, 1049–1061.
(16) Zimmerman, S. B.; Minton, A. P. Macromolecular crowding - Biochemical, Biophysical, and Physiological consequences. *Annu. Rev. Biophys. Biomol. Struct.* **1993**, *22*, 27–65.
(17) Minton, A. P. Macromolecular crowding. *Curr. Biol.* **2006**, *16*, R269–R271.
(18) Zhou, H. X.; Rivas, G. N.; Minton, A. P. Macromolecular crowding and confinement: Biochemical, Biophysical, and potential physiological consequences. *Annu. Rev. Biophys.* **2008**, *37*, 375–397.
(19) Mittal, J.; Best, R. B. Thermodynamics and kinetics of protein folding under confinement. *Proc. Natl. Acad. Sci. U.S.A.* **2008**, *1051*, 20233–20238.
(20) Vlachy, V. Correlations between macroions in mixtures of charged and uncharged macroparticles. *J. Chem. Phys.* **1993**, *99*, 471–476.
(21) Vlachy, V.; Bhuiyan, L. B.; Outhwaite, C. W. Asymmetric electrolyte in mixture with a neutral component: elects of counterion charge. *Mol. Phys.* **1997**, *90*, 553–561.
(22) Reščič, J.; Vlachy, V.; Bhuiyan, L. B.; Outhwaite, C. W. Monte Carlo simulation studies of electrolyte in mixture with a neutral component. *J. Chem. Phys.* **1997**, *107*, 3611–3618.
(23) Reščič, J.; Vlachy, V.; Bhuiyan, L. B.; Outhwaite, C. W. Monte Carlo simulations of a mixture of an asymmetric electrolyte and a neutral species. *Mol. Phys.* **1998**, *95*, 233–242.
(24) Reščič, J.; Vlachy, V.; Outhwaite, C. W.; Bhuiyan, L. B.; Mukherjee, A. K. A Monte Carlo simulation and symmetric Poisson-Boltzmann study of a four-component electrolyte mixture. *J. Chem. Phys.* **1999**, *111*, 5514–5521.
(25) Bhuiyan, L. B.; Vlachy, V.; Outhwaite, C. W. Understanding polyelectrolyte solutions: macroion condensation with emphasis on the presence of neutral co-solutes. *Int. Rev. Phys. Chem.* **2002**, *21*, 1–36.
(26) Molero, M.; Outhwaite, C. W.; Bhuiyan, L. B. Individual Ionic Activity Coefficients from a Symmetric Poisson-Boltzmann Theory. *J. Chem. Soc., Faraday Trans.* **1992**, *88*, 1541–1547.
(27) Outhwaite, C. W. *Statistical Mechanics*, Vol. II, Specialist Periodical Report; The Chemical Society: London, 1975; pp 188−255.
(28) Outhwaite, C. W. A modified Poisson-Boltzmann approach to homogeneous ionic solutions. *Condens. Matter Phys.* **2004**, *7*, 719–733.
(29) Hansen, J.-P.; McDonald, I. R. *Theory of Simple Liquids*, 2nd ed.; Academic Press: New York, 1990.
(30) Lamperski, S.; Płuciennik, M. The activity coefficient of high density systems with hard-sphere interactions: the application of the IGCMC method. *Mol. Simul.* **2010**, *36*, 111–117.
(31) Blum, L. *Theoretical Chemistry, Advances and Perspectives*, Vol. 5; Eyring, H., Henderson, D., Eds.; Academic Press: New York, 1980; pp 1−66.
(32) Leonard, P. J.; Henderson, D.; Barker, J. A. Calculation of radial distribution function of hard-sphere mixtures in Percus-Yevick approximation. *Mol. Phys.* **1971**, *21*, 107–111.
(33) Grundke, E. W.; Henderson, D. Distribution functions of multicomponent fluid mixtures of hard-spheres. *Mol. Phys.* **1974**, *24*, 269–281.
(34) Verlet, L.; Weis, J. J. Equilibrium theory of simple liquids. *Phys. Rev. A* **1972**, *5*, 939–952.
(35) Outhwaite, C. W.; Molero, M.; Bhuiyan, L. B. Primitive Model Electrolytes in the Modified Poisson-Boltzmann Theory. *J. Chem. Soc., Faraday Trans.* **1993**, *89*, 1315–1320. Corrigendum, *ibid* **1994**, *90*, 2002.
(36) Perram, J. W. Hard sphere correlation functions in the Percus-Yevick approximation. *Mol. Phys.* **1975**, *30*, 1505–1509.
(37) Baxter, R. J. Ornstein-Zernike Relation and Percus-Yevick Approximation for Fluid Mixtures. *J. Chem. Phys.* **1970**, *52*, 4559–4562.
(38) Ebeling, W.; Scherwinski, K. On the estimation of theoretical individual activity coefficients of electrolytes. *Z. Phys. Chem. (Leipzig)* **1983**, *264*, 1–14.

(39) Vlachy, V.; Hribar-Lee, B.; Bhuiyan, L. B. Mean Activity Coefficient of a Simple Electrolyte, Dissolved in the Presence of an Arbitrary Number of Cosolute Components. *J. Chem. Eng. Data* **2010**, *55*, 1855–1859.

(40) Vlachy, V.; Ichiye, T.; Haymet, A. D. J. Symmetric Strong Electrolytes: GCMC Simulation and Integral Equations. *J. Am. Chem. Soc.* **1991**, *113*, 1077–1082.

(41) Belloni, L. A Hypernetted Chain Study of Highly Asymmetrical Polyelectrolytes. *Chem. Phys.* **1985**, *99*, 43–54.

(42) Corti, H. R. Prediction of Activity Coefficients in Aqueous Electrolyte Mixtures using the Mean Spherical Approximation. *J. Phys. Chem.* **1987**, *91*, 686–689.

(43) Sanchez-Castro, C.; Blum, L. Explicit approximation for the Unrestricted Mean Spherical Approximation for Ionic Solutions. *J. Phys. Chem.* **1989**, *93*, 7478–7482.

(44) Lamperski, S. Individual and mean activity coefficients of an electrolyte from the inverse GCMC simulation. *Mol. Simul.* **2007**, *33*, 1193–1198.

(45) Asakura, F.; Oosawa, F. Surface Tension of High-Polymer Solutions. *J. Chem. Phys.* **1954**, *22*, 1255.

Received for review April 21, 2010. Accepted June 11, 2010. L.B.B. acknowledges an institutional grant through Fondos Institucionales Para la Investigación (FIPI), University of Puerto Rico. V.V. and B.H.-L. acknowledge the support of the Slovenian Research Agency fund (Program 0103-0201). V.V. is the Adjunct Professor at the University of California, Department of Pharmaceutical Chemistry.

JE100394D